Spatial entanglement of formation in pure and mixed energy states of identical non-interacting massive bosons

R A W Bradford
1 Merlin Haven, Wotton-under-Edge, Glos.GL12 7BA, UK

E-mail: rick.bradford@british-energy.com

Abstract. The entanglement of formation (EoF) between one-dimensional spatial regions is calculated for one, two and three identical, non-interacting, non-relativistic bosons. Both pure energy eigenstates and mixed states of up to 13 energy eigenstates are addressed. Particular cases are thermal states. The EoF is found to diminish as inverse temperature to a power between 0.5 and 0.63 in 1D. The EoF is also evaluated for mixtures of energy states which are quite different from thermal states. This sheds some light on the reason why the EoF reduces with increasing temperature. This is not due to increasing mixity alone, but also because of the preponderance within a thermal mixture of consecutive energy states, i.e. states differing in quantum number by 1. In contrast, the EoF remains high even for large mixities if all contributing pairs of quantum numbers differ by more than 1. In particular, the EoF is maximal if all contributing states have the same parity, even for maximal mixity. Hence, infinite sub-mixtures of thermal states, with maximal mixity, can also have maximal EoF, even at high temperatures when the thermal state itself has vanishing entanglement. The spatial EoF is maximised when the partition splits the region of confinement into halves. For N bosons in the same energy state a good approximation to the EoF for a 50/50 partition is $1 + 0.5\log_2 N$. This provides an upper bound to the spatial EoF which can be obtained from a BEC. For example, a million atoms in the condensed phase produce an EoF of only 11 ebits. The spatial EoF for N bosons in a pure state with differing energies always exceeds that for equal energies. The upper bound for the spatial EoF of N bosons in a pure state with differing energies is N ebits, which contrasts sharply with the EoF for equal energies. The upper bound of N ebits is realised in the case of states of equal parity and a 50-50 partition.

PACS numbers: 03.65.Ud, 05.30.Jp
Submitted to: None – long preprint version only

1. Introduction

The entanglement of quantum systems has been a vigorous area of research for the last fifteen years. This has been stimulated by the realisation that entanglement is the essential ingredient in many applications in quantum communication, [1], quantum teleportation, [2], quantum cryptography, [3,4,5], and quantum computing [6,7]. However, a motivation of longer standing is the appreciation that entanglement is necessary for the logical coherence of quantum mechanics. The resolution of the EPR problem, [8], is the archetypal example. Perhaps the simplest example, however, is to consider a single particle described by a broad Schrodinger wavepacket. Using two detectors at a space-like separation, there would appear to be a non-zero probability of both detectors registering the presence of the same particle. Of course there is not, and the resolution of this conundrum which also avoids acausal behaviour is to recognise that the spatially separated regions are entangled, even when only a single particle is involved. The further implication of this example is that the correct quantum description is the quantum field.

Entanglement is not an intrinsic property of a quantum system, as emphasised in [9]. Entanglement exists only with respect to a given partition of the system into component parts. Specifically it must be possible to express the Hilbert space in question as the direct product of the Hilbert spaces of constituents, $H = H_A \otimes H_B$. With respect to this particular partition a given pure state is said to be separable if and only if it can be written as the direct product of A and B states, i.e., $|\psi\rangle = |a\rangle_A \otimes |b\rangle_B$, where $|a\rangle_A \in H_A$ and $|b\rangle_B \in H_B$. A state which cannot be so factorised is said to be entangled with respect to the partition $H = H_A \otimes H_B$.

It is not mere pedantry to insist that the partition in question is clearly defined. For a given quantum system, one may discuss many different types of entanglement depending upon how the composite system has been chosen to be partitioned. Failure to identify clearly what partition is intended can lead to confusion. It has been shown, for example, that any state vector $|\psi\rangle$ in any Hilbert space of non-prime dimension is separable with respect to a suitably chosen partition, [9]. The partition in which a composite state is separable is not necessarily the most obvious one. For example, considering a hydrogen atom to be composed of a proton and an electron is a partition in which the hydrogen atom is entangled, [10], albeit to only a small degree due to the disparity of its constituents' masses. The partition which disentangles the hydrogen atom and provides a separable state is the combination of the atom's centre of mass and the 'relative particle' with mass equal to the reduced mass, [10].

A further example is provided by a system of identical, non-interacting bosons. Suppose we consider a particle based partition in which $|i\rangle_j$ represents the jth particle in the ith quantum state (perhaps an energy eigenstate in a confining potential). A state of N particles can then be represented by a direct product of such states, one for each particle, together with such symmetrisation as may be required. If the bosons are all in the same state, as happens in the BEC phase, the N particle state is the direct product $|g\rangle_1 |g\rangle_2 ... |g\rangle_N$, where g represents the ground state. Hence, the BEC phase is separable with respect to a partition into particles.

However, another possible partition is the spatial partition which results from the field description. In this case the objects whose states form the component parts are not the particles but spatial regions. For example, a region of confinement may be divided into two parts, denoted by the subscripts $_A$ and $_B$. The Hilbert space of the system may be expressible as a direct product of the Hibert spaces of these spatial parts which in general may be entangled. For example, if there were just a single particle present, a possible state after tracing out unwanted details is $\left(|0\rangle_A |1\rangle_B + |1\rangle_A |0\rangle_B\right)/\sqrt{2}$, where the number denotes the occupancy of the region. This state is spatially entangled. Spatial entanglement of this sort arises naturally below the BEC transition temperature, [11,12,13,14,33,34], essentially because of the dominance of a single energy eigenstate. The hypothesised association between spatial entanglement and the long range order characteristic of phase transitions has been another recent incentive to the study of entanglement.

Clearly, there can be no entanglement with respect to a partition into particles when only one particle is present. However, the partition into spatial regions is just as valid for one particle as for many, so the potential for spatial entanglement exists for one particle systems, [9,15]. The suggestion that the entanglement of single particle systems should be experimentally detectable probably remains controversial, criticisms of early proposals being given in [16,17,18]. However, schemes to detect single particle entanglement unambiguously continue to be devised and attempted, e.g. [19,20,21,40], but are so far probably not free of loopholes.

As regards the spatial entanglement between many particle systems, the theoretical existence has been demonstrated of entanglement between spins, or individual oscillators, in thermal states on a1D lattice, e.g. [22,23]. However, these are not true examples of 'spatial entanglement' since the entanglement actually exists between individual atoms/oscillators which happen to be spatially defined. In this paper, however, we are interested in true spatial

entanglement, i.e. the entanglement between a quantum field at two locations, such as has been discussed in [11,12,13,14,33,34]. Schemes which are claimed to be capable of experimentally detecting true spatial entanglement have been devised, e.g. [24], but confirmation of its physical importance remains to be seen.

Quantification of the degree of entanglement has been widely discussed, e.g., [25,26,27,28]. Many different measures are available, but often present computational difficulties, especially for mixed states. The entanglement of formation, [29], which will be employed here, is generally agreed to be one suitable quantitative measure of entanglement. For pure quantum states of a composite system, the entanglement of formation is defined as the von Neumann entropy of the reduced density matrix of one component part. Thus, if $|\psi\rangle$ is the state of the composite system, then $EoF = S_{vN}(\hat{\rho}_A)$, where $\hat{\rho}_A = Tr_B(|\psi\rangle\langle\psi|) = \sum_{b\in B}\langle b|\psi\rangle\langle\psi|b\rangle$, where A and B are the components parts, and $S_{vN}(\hat{\rho}_A) \equiv -Tr[\hat{\rho}_A \log_2 \hat{\rho}_A]$. Note that we shall use $\log_2$ in the definition of entanglement throughout this paper, rather than adopting a varying base according to the dimension of the Hilbert space, as do some authors. The advantage of this is that the entanglement of formation (EoF) then has an absolute meaning and the entanglement of states from Hilbert spaces of differing dimension can be compared. The unit of entanglement is that of a two qubit Bell state, or singlet state (one ebit).

The EoF may be easy to evaluate directly from its definition for any explicitly defined pure quantum state. However, the situation is different for mixed states. The density matrix, $\hat{\rho}$, defining a mixed state will have many possible decompositions into explicit mixtures of pure states, $|\psi_i\rangle$. That is, there will be many ways in which to express the density matrix as $\hat{\rho} = \sum_i p_i |\psi_i\rangle\langle\psi_i|$, where the p_i are real probabilities in the range [0,1] and the states $|\psi_i\rangle$ are normalised but otherwise arbitrary and need not be orthogonal or linearly independent. The average entanglement of this specific decomposition is defined as the average of the entanglements of its pure states, $E_{av} = \sum_i p_i EoF(|\psi_i\rangle)$. But the value of E_{av} depends upon the decomposition, and hence cannot be the true entanglement in general, since this depends only upon the density matrix and the chosen partition. The entanglement of formation is defined as the minimum value of E_{av} for any decomposition, $EoF = MIN_{\{|\psi_i\rangle\}}(E_{av})$.

The definition of the EoF is uncontentious but unfortunately provides difficulties as regards explicit computation in the general case. A closed form expression for the EoF has been given in [30,31] for the case of an arbitrary mixture of two qubits. Simple expressions have also been found for isotropic states (the class of density matrices which are convex mixtures of a maximally entangled state and the maximally mixed state), [32]. However, the general case remains a challenge to evaluate. In this paper, the EoF of density matrices of dimension greater than 2 x 2 has been evaluated by numerical optimisation (see the Appendix).

2. Purpose, overview and structure of the paper

In this paper we evaluate the spatial EoF for systems of one, two or three identical, non-relativistic, non-interacting bosons. (The cases of single particles may equally be regarded as fermions). Pure states of definite energy are addressed as well as mixtures of such states. The energy eigenstates are defined with respect to a confining potential, or box, and the calculations are restricted to the 1D case. The formulation of the problem is described in Section 3.

There were several motivations for this work. The first was to clarify the dependence of spatial EoF on the size, position and spacing of the regions defining the partition. These issues are illustrated here using the simplest possible case: a single particle in a pure energy eigenstate (Section 4). The second motivation was to gain greater understanding of how the spatial EoF changes with increasing mixity, and how the specific energy states in the mixture affect this. To

this end the spatial EoF of mixtures of between 2 and 10 energy states are calculated for a single particle (Section 5). This permits the special case of thermal mixtures to be addressed for a single particle, illustrating the reduction in EoF with increasing temperature (Section 6). A third motivation was to understand how particle number influences the EoF. Some observations are made regarding the N particle spatial EoF for pure energy states, distinguishing particularly between the cases when all particles are in the same energy eigenstate and when all particles are in different energy eigenstates (Sections 7,8). The EoF is calculated explicitly for pure states of two and three particles in differing energy eigenstates (Sections 8,9). Finally, the EoF is calculated for mixed energy states of two particles approximating the thermal state (Section 10).

A final motivation was to understand the absolute total spatial EoF in these states. Whilst spatial entanglement in systems of free bosons has been calculated before, e.g. [11,12,13,14,33,34], this has been restricted to quantification via the negativity, [35], or by purity measures, [14,28]. In effect these entanglement witnesses are restricted to quantifying the entanglement of just a single mode, and hence are all of order unity or less despite the many-particle systems considered. In contrast, here we address the total entanglement of formation.

3. Formulation of partitioned states

Numerical examples will be restricted to the 1D case and hence the formulation below is also restricted to 1D, though it generalises to 3D in a straightforward manner. We consider non-relativistic, non-interacting bosons confined either through some central potential or within a box. The potential, $V(x)$, is assumed to be sufficient to produce bound states. The energy eigenfunctions of the Hamiltonian, $\hat{H} = -\hbar^2 \partial_x^2 / 2m + V(x)$, are denoted $u(n,x)$. To simplify the numerical examples, the potential is required to be symmetrical, i.e. an even function, $V(-x) = V(x)$. Consequently the energy eigenstates, $u(n,x)$, have definite parity. The potential is also assumed to produce an infinite set of bound state eigenfunctions which are orthonormal and complete. Examples include a harmonic potential or box confinement. The latter case will be used in numerical examples, although not necessary for the general development. We shall refer to the total spatial region as a 'box' for convenience, but this may be infinite space. The box modes are $u(n,x) = \sqrt{\frac{2}{L}} \sin\left(\frac{n\pi x'}{L}\right)$, where $x' = x + L/2$, which vanish at the box walls, $x = \pm L/2$.

In terms of a Fock basis, a quantum field operator is $\hat{\psi}(x) = \sum_{n=1}^{\infty} u(n,x)\hat{a}_n$. Formulation of the partitioned states broadly follows [11]. The creation operator for a mode specified by $f(x)$ can be written $\hat{f}^+ = \int_{Box} f(x)\hat{\psi}^+(x).dx$ and f is assumed normalised, $\int_{Box} |f(x)|^2 dx = 1$. A normalised state of a single particle in this mode is then $\hat{f}^+|0\rangle$. Now consider the box to consist of three spatial partitions, labelled A, B and O. For region A, the mode function is modified such that its support is A. Hence the creation operator for a particle in this mode, and hence in region A, is $\hat{f}_A^+$, where,

$$\alpha \hat{f}_A^+ = \int_{x \in A} f(x)\hat{\psi}^+(x).dx \qquad (1)$$

The constant, α, is defined so that $\hat{f}_A^+|0\rangle$ is a normalised state representing a single particle in this mode in region A. Hence we require, $|\alpha|^2 = \int_{x \in A} |f(x)|^2 dx$. Creation operators for regions B

and O are defined analogously. Now choosing *f(x) = u(n,x)*, we have,

$$\hat{f}^{+} \to \hat{a}_n^{+} = \alpha_n^A \hat{a}_{An}^{+} + \alpha_n^B \hat{a}_{Bn}^{+} + \alpha_n^O \hat{a}_{On}^{+} \tag{2}$$

where,
$$\hat{a}_{An}^{+} = \frac{1}{\alpha_n^A} \sum_{k=1}^{\infty} R_{nk}^A \hat{a}_k^{+} \tag{3}$$

and,
$$R_{nk}^A \equiv \int_{x \in A} u(n,x) u(k,x)^{*} dx \,, \tag{4}$$

and,
$$\left|\alpha_n^A\right|^2 = \sum_{k=1}^{\infty} \left|R_{nk}^A\right|^2 = \int_{x \in A} \left|u(n,x)\right|^2 dx \tag{5}$$

The latter expression follows from the completeness relation for the eigenfunctions, $\sum_{k=1}^{\infty} u(k,x)^{*} u(k,y) = \delta(x-y)$, which also gives $\sum_{k=1}^{\infty} R_{mk}^{A*} R_{nk}^A = R_{nm}^A$. Equation (5) also holds for the other regions, with A replaced by B or O. The commutation relations between the partitioned creation and annihilation operators are,

$$\left[\hat{a}_{An}^{+}, \hat{a}_{Ak}^{+}\right] = \left[\hat{a}_{An}^{+}, \hat{a}_{Bk}^{+}\right] = \left[\hat{a}_{An}, \hat{a}_{Ak}\right] = \left[\hat{a}_{An}, \hat{a}_{Bk}\right] = \left[\hat{a}_{Am}, \hat{a}_{Bn}^{+}\right] = 0 \tag{6}$$

The last of these follows from $\int_{x \in A} dx \int_{y \in B} dy\, u_n(x) u_m(y)^{*} \delta(x-y) \equiv 0$. However, the distinction between the partitioned operators and the true Fock operators results from the final commutator,

$$S_{nm}^A \equiv \left[\hat{a}_{An}, \hat{a}_{Am}^{+}\right] = \frac{1}{\alpha_n^{A*} \alpha_m^A} \sum_{k=1}^{\infty} R_{nk}^{A*} R_{mk}^A = \frac{R_{mn}^A}{\alpha_n^{A*} \alpha_m^A} \tag{7}$$

This is unity when $n = m$, i.e. $S_{nn}^A = 1$, consistent with Fock space, $\left[\hat{a}_m, \hat{a}_n^{+}\right] = \delta_{nm}$. However, unlike the latter, (7) is also non-zero in general for $n \neq m$. It is this latter fact that gives the partition its non-trivial structure and leads to the entanglement of formation falling below its maximum possible value in certain cases.

The Fock states for the whole box are,

$$\left| N_1(k_1), N_2(k_2), ... \right\rangle \equiv \frac{\left(\hat{a}_{k_1}^{+}\right)^{N_1}}{\sqrt{N_1!}} \cdot \frac{\left(\hat{a}_{k_2}^{+}\right)^{N_2}}{\sqrt{N_2!}} ..... \left| 0 \right\rangle \tag{8}$$

Analogously we can define partitioned states with respect to the A, B and O regions by,

$$\xi \left| N_1(k_1), N_2(k_2), ... \right\rangle_A \equiv \frac{\left(\hat{a}_{Ak_1}^{+}\right)^{N_1}}{\sqrt{N_1!}} \cdot \frac{\left(\hat{a}_{Ak_2}^{+}\right)^{N_2}}{\sqrt{N_2!}} ..... \left| 0 \right\rangle \tag{9}$$

and similarly with A replaced by B or O. However, caution is needed when dealing with these partitioned states since they are not all mutually orthogonal. Indeed, they would not all be normalised, either, were it not for the introduction of the ξ coefficient. Partitioned states of N particles all in the same energy eigenstate, k, i.e.,

$$\left| N(k) \right\rangle_A \equiv \frac{\left(\hat{a}_{Ak}^{+}\right)^{N}}{\sqrt{N!}} \cdot \left| 0 \right\rangle \tag{10}$$

are normalised and mutually orthogonal. Hence, $\xi = 1$ in these cases. However, the partitioned states of two or three particles of differing energy require $\xi > 1$ in order to be normalised in

general. For the states $|nm\rangle_A \equiv |1(n),1(m)\rangle_A$ and $|nmq\rangle_A \equiv |1(n),1(m),1(q)\rangle_A$, where n, m and q are all different, normalisation requires $\left|\xi^A_{nm}\right|^2 = \langle 0|\hat{a}_{Am}\hat{a}_{An}\hat{a}^+_{An}\hat{a}^+_{Am}|0\rangle$ and $\left|\xi^A_{nmq}\right|^2 = \langle 0|\hat{a}_{Aq}\hat{a}_{Am}\hat{a}_{An}\hat{a}^+_{An}\hat{a}^+_{Am}\hat{a}^+_{Aq}|0\rangle$. Repeated use of the commutation relation, (7), leads to,

$$\left|\xi^A_{nm}\right|^2 = 1 + \left|S^A_{nm}\right|^2 \tag{11}$$

$$\left|\xi^A_{nmq}\right|^2 = 1 + 2\Re\left(S^A_{nm}S^A_{nq}S^A_{mq}\right) + \left[\left|S^A_{nm}\right|^2 + \left|S^A_{nq}\right|^2 + \left|S^A_{mq}\right|^2\right] \tag{12}$$

Two single-particle partitioned states in different energy states, $|n\rangle_A \equiv |1(n)\rangle_A$ and $|m\rangle_A \equiv |1(m)\rangle_A$, are not orthogonal in general. In fact,

$${}_A\langle n|m\rangle_A = \langle 0|\left[\hat{a}_{An}, \hat{a}^+_{Am}\right]|0\rangle = S^A_{nm} \tag{13}$$

Similarly, a pair of two-particle states, say $|nq\rangle_A$ and $|nm\rangle_A$, will not in general be orthogonal, as reduction of ${}_A\langle nm|nq\rangle_A = \langle 0|\hat{a}_{Am}\hat{a}_{An}\hat{a}^+_{An}\hat{a}^+_{Aq}|0\rangle$ using the commutation relations shows. All the above relations apply equally with region A replaced by B or O. Partitioned states for one region are all orthogonal to partitioned states for another region. Partitioned states of N particles are orthogonal to any partitioned state of a differing number of particles.

Since the states $u(n,x)$ have definite parity, we may assume that the states are labelled so that their parity is $(-1)^{n-1}$. The implication of this for a partition into regions A and B which are each half of the box is that all of the $\left|\alpha^{A,B}_n\right|^2 = ½$ and $S^{A,B}_{nm} = R^{A,B}_{nm} = 0$ whenever n and m have the same parity. The latter follows from orthogonality of the eigenstates $\int u(n,x)^* u(m,x)dx = \delta_{nm}$ and the fact that the integral receives equal contributions from both halves of the box when the parities are the same.

4. Spatial EoF for a single particle in a pure energy state

Despite its simplicity, this example provides insight into the dependence of the spatial EoF on the size, position, and gap between, the spatial regions. The vacuum is written as the direct product of the vacuum for each part: $|0\rangle_A|0\rangle_B|0\rangle_O$. Hence (2) gives,

$$|n\rangle = \alpha^A_n|n\rangle_A|0\rangle_B|0\rangle_O + \alpha^B_n|0\rangle_A|n\rangle_B|0\rangle_O + \alpha^O_n|0\rangle_A|0\rangle_B|n\rangle_O \tag{14}$$

It is clear from (14) that the energy eigenstates will in general be entangled with respect to this spatial partition. Suppose we are interested in the bipartite entanglement between regions A and B. We are thus interested in the density matrix formed by tracing out the state of the "other" region, O, which gives,

$$\hat{\rho}_{AB} = Tr_O\left(|n\rangle\langle n|\right) = |\chi\rangle\langle\chi| + \left|\alpha^O_n\right|^2|0\rangle_A|0\rangle_B\langle 0|_A\langle 0|_B \tag{15}$$

where,
$$|\chi\rangle = \alpha^A_n|n\rangle_A|0\rangle_B + \alpha^B_n|0\rangle_A|n\rangle_B \tag{16}$$

In terms of a 2 x 2 bipartite basis with matrix indices in the order $|0\rangle_A|0\rangle_B$, $|0\rangle_A|n\rangle_B$, $|n\rangle_A|0\rangle_B$, $|n\rangle_A|n\rangle_B$, the density matrix is,

$$(\rho_{AB}) = \begin{pmatrix} \left|\alpha_n^O\right|^2 & 0 & 0 & 0 \\ 0 & \left|\alpha_n^{\mathbf{B}}\right|^2 & \alpha_n^{A*}\alpha_n^B & 0 \\ 0 & \alpha_n^A\alpha_n^{B*} & \left|\alpha_n^A\right|^2 & 0 \\ 0 & 0 & 0 & 0 \end{pmatrix} \tag{17}$$

noting that $\sum_{I=A,B,C}\left|\alpha_n^I\right|^2 = 1$, as required. Since this is a 2 x 2 bipartite density matrix, the EoF may be found using the closed form solution of [30,31]. The resulting EoF has been calculated for the case of a particle confined in a box and illustrated in figure 1 (for n = 1). In this illustration the regions A and B are of the same size and symmetrically disposed about the box centre, in general with a gap between them. The same results are obtained whether the box is one dimensional or three dimensional so long as the regions A and B both extend over the whole of the y and z widths of the box in the latter case. Figure 1 plots the EoF against the length of the regions (as a proportion of the box width). When A and B are each half of the box, the EoF is unity. This is true for all pure energy states as may be seen from the reduced density matrix which is $\begin{pmatrix} \left|\alpha_n^B\right|^2 & 0 \\ 0 & \left|\alpha_n^A\right|^2 \end{pmatrix}$ and this becomes $\frac{1}{2}\begin{pmatrix} 1 & 0 \\ 0 & 1 \end{pmatrix}$ for a half-and-half partition. This is true for an arbitrary symmetrical confining potential, $V(x)$. The EoF reduces if the A and B regions are reduced in size, or the gap between them is increased. For other pure energy states, e.g. n = 2, the dependence of the EoF on the gap is more complex and need not be monotonic. This is simply because the EoF tends to be greater if the magnitudes of the $\alpha_n^{A,B}$ coefficients are larger – and this depends on what positioning of the A and B regions captures the most probability density, see (5). Note that the absence of a dependence on the gap reported in [11] is a consequence of the free space (plane wave) normalisation used in [11]. In general there will be a gap dependence for confined particles since the magnitudes of the $\alpha_n^{A,B}$ coefficients depend upon the positioning of the A and B regions, even for a given length.

5. Single particle in equal mixtures of energy eigenstates

5.1 Orthogonalisation procedure

In this investigation we assume throughout that the regions A and B are each half of the box (region O vanishes). Hence, for a pure energy state the EoF would be unity (see Section 4). We also confine attention in this Section to equal mixtures such that each of N_S different energy states contribute with probability, $1/N_S$. The density matrix for an equal mixture of the energy states n_1, n_2,… is,

$$\hat{\rho} = \frac{1}{N_S}\sum_{i=1}^{N_S}\left|n_i\right\rangle\left\langle n_i\right| \tag{18}$$

Each energy eigenstate can be written in the form,

$$\left|n_j\right\rangle = \alpha_{n_j}^A\left|n_j\right\rangle_A\left|0\right\rangle_B + \alpha_{n_j}^B\left|0\right\rangle_A\left|n_j\right\rangle_B \tag{19}$$

$$\left|\alpha_{n_j}^{A,B}\right|^2 = \int_{x\in A,B}\left|u(n_j,x)\right|^2 dx \tag{20}$$

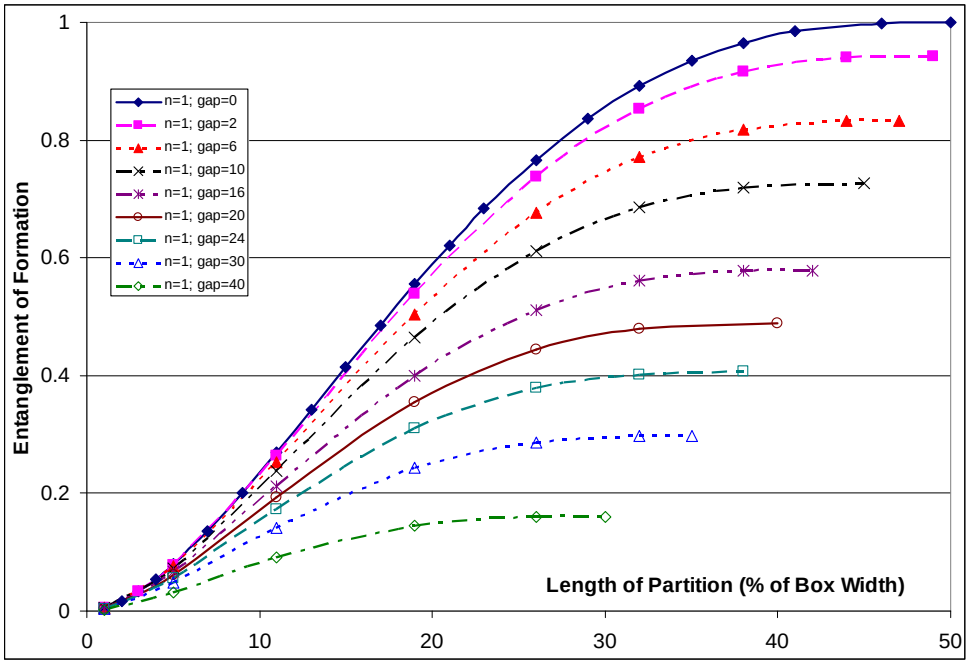

Figure 1. Spatial EoF of a single particle in the ground state versus the length of the partitions for various gaps between the partitions and with the gap centred on the middle of the box.

We have written (19) with arbitrary α coefficients but we consider only $\left|\alpha_j^{A,B}\right|^2 = ½$ in the numerical examples, i.e. the box is partitioned into equal halves. Because the partitioned states $\left\{\left|n_j\right\rangle_{A,B}\right\}$ are not orthonormal, we need to introduce an orthonormalizing scheme before attempting to find the EoF numerically. The orthonormalized single-particle A-partition states are denoted $\left\{\left|\psi_j^A\right\rangle\right\}$. In terms of these the $\left|n_j\right\rangle_A$ states are written,

$$\left|n_j\right\rangle_A = \sum_{k=1}^{j} C_{jk}^A \left|\psi_k^A\right\rangle \tag{21}$$

Similarly, the B-system states are written $\left|n_j\right\rangle_B = \sum_{k=1}^{j} C_{jk}^B \left|\psi_k^B\right\rangle$. The first of the basis vectors is just,

$$\left|\psi_1^{A,B}\right\rangle = \left|n_1\right\rangle_{A,B} \tag{22}$$

For j > 1, orthonormality gives the first coefficient in (21) as,

$$C_{j1}^A = {}_A\!\left\langle n_1 \middle| n_j \right\rangle_A = S_{[1j]}^A \tag{23}$$

where for clarity we have introduced the notation $S_{[pq]}^A$ to stand for S_{KL}^A evaluated at $K = n_p$ and $L = n_q$. The remaining coefficients are found by successively forming the scalar product of (21) with each state $\left|\psi_k^A\right\rangle$ in turn. This leads to the following general expression which applies for 1 < k < j,

$$C_{jk}^A = \frac{1}{C_{kk}^{A*}}\left[S_{[kj]}^A - \sum_{i=1}^{k-1} C_{ki}^{A*} C_{ji}^A\right] \tag{24}$$

The last coefficient for each 'j' is given by,

$$C_{jj}^{A} = \sqrt{1 - \sum_{k=1}^{j-1} \left| C_{jk}^{A} \right|^2} \tag{25}$$

Note that (24) involves finding the kth coefficient for the jth state in terms of, (a)the ith coefficients of the jth state, with i < k and which have thus already been found, and, (b)the coefficients for the kth states with k < j, which have also already been found. Thus the only additional evaluation required for each new C_{jk}^{A} is the scalar product $S_{[kj]}^{A}$ from (4,5,7). Equations (23,24,25) apply equally with A replaced throughout by B.

The orthonormalization scheme of (21-25) result in the N_S energy states, (19), being expressible in terms of N_S+1 A-system states and N_S+1 B-system states. These states are the A-vacuum, $\left|0\right\rangle_A$, and the N_S occupied A-states, $\left|\psi_j^A\right\rangle$, plus the B-system equivalents. Hence, the density matrix for a mixture of N_S distinct energy states is a special case of an (N_S+1) × (N_S+1) bipartite density matrix.

5.2 Mixtures of equal parity energy states

If all the energy states contributing to the mixture have the same parity, and a 50/50 partition is considered, then $S_{nm}^{A,B} = 0$ for all pairs of states with $n \neq m$, and the C-coefficients become simply $C_{jk}^{A,B} = 0$ except for $C_{jj}^{A,B} = 1$. The original partitioned states $\left\{\left|n_j\right\rangle_{A,B}\right\}$ are already orthonormal in this case, $\left|1\right\rangle = \frac{1}{\sqrt{2}}\left\{\left|1\right\rangle_A\left|0\right\rangle_B + \left|0\right\rangle_A\left|1\right\rangle_B\right\}$, $\left|2\right\rangle = \frac{1}{\sqrt{2}}\left\{\left|2\right\rangle_A\left|0\right\rangle_B + \left|0\right\rangle_A\left|2\right\rangle_B\right\}$, etc. It is simple to show that any mixture of such states gives unit entanglement. The restriction to just odd or even parity states can be envisaged as placing a boundary in the middle of the box, with suitable boundary conditions imposed (Dirichlet for odd parities, Neumann for even parities). In either case we end up with a set of states which are orthogonal not just over the whole box but also over each half-box. So the partitioned energy states form an orthonormal basis.

5.3 Numerical results for the EoF of single-particle mixed states

The EoF has been evaluated using the numerical method described in the Appendix for two, three and four state mixtures of a single particle and for a range of quantum numbers. The results are listed in tables 1, 2 and 3 respectively. The minimum EoF for a given N_S is the state of lowest mean energy, i.e. the mixture with consecutive energy states starting with the ground state, n_1 = 1, n_2 = 2,etc. Of the cases evaluated, that with the second lowest EoF had quantum numbers (3,4,5…). Hence, energy is no guide to the EoF after the lowest energy state.

The entries shown in italics (online red text) in tables 1-3 are those for which all the quantum numbers n_i differ by more than 1. It is striking that these are also the cases for which EoF > 0.9. If any pair of quantum numbers differ by 1, then EoF < 0.9, otherwise the EoF > 0.9. Thus, the spatial entanglement between the two halves of a box confining a single particle which is equally likely to occupy any energy state chosen from a set which all differ in quantum number by >1, is little less than the maximal value of one ebit. Despite the elementary nature of the analysis, this result is nontrivial – even rather surprising. As noted in Section 5.2, if all the quantum numbers, n_i, have the same parity then the EoF is unity.

Does additional mixity lead to a reduction in entanglement? Consider firstly adding a third state to a two-state mixture. It certainly is *not* the case that adding the third energy component automatically reduces the entanglement. For example, consider n_1=1 and n_2=2. The entanglement of this two energy mixed state is 0.3862. However, we see that adding a third energy component with n_3>3 leads to an entanglement of ≥0.5033, i.e. the entanglement is larger for the three-energy state. The reason for this, however, is that the n_1=1 and n_2=2 combination has a particularly low entanglement. In the three energy state with n_1=1, n_2=2 and n_3=4 (say), we might equally well have considered the pairs n_2=2 and n_3=4 (with unit

entanglement) or n_1=1 and n_3=4 (with entanglement 0.9151), with respect to which the three energy state has reduced entanglement. This suggests that the best comparison might be with the pair-wise average entanglement. For example, for n_1=1, n_2=2 and n_3=4, the pair-wise average entanglement of the three energy state would be (0.3862 + 1 + 0.9151)/3 = 0.7671, with respect to which the actual three energy state entanglement is reduced (i.e. 0.5033 < 0.7671).

Table 1. Equal mixtures of two energy states (n,m) for a single particle and a 50/50 partition. Italic (red online) text indicates states with quantum numbers which differ by >1.

n	m	EoF
1	2	0.3862
1	*4*	*0.9151*
1	*6*	*0.9653*
1	*8*	*0.981*
2	3	0.8039
2	*5*	*0.9894*
2	*7*	*0.9977*
3	4	0.5740
3	*6*	*0.9413*
3	*8*	*0.9750*
4	5	0.7549
4	*7*	*0.9828*
4	*9*	*0.9956*
5	6	0.6163
5	*8*	*0.9501*
5	*10*	*0.9790*
odd	*odd*	*1*
even	*even*	*1*

Table 2. Equal mixtures of three energy states (n,m,q) for a single particle and a 50/50 partition. Italic (red online) text indicates states with quantum numbers which differ by >1.

n	m	q	EoF
1	2	3	0.3638
1	2	4	0.5033
1	2	5	0.5803
1	3	4	0.6426
1	*3*	*6*	*0.9371*
1	4	5	0.7719
1	*4*	*6*	*0.9192*
1	*4*	*7*	*0.9314*
2	3	4	0.5406
2	3	5	0.8615
2	3	6	0.8259
2	3	7	0.8676
2	4	5	0.8286
2	*4*	*7*	*0.9870*
2	5	6	0.7355
2	*5*	*7*	*0.9914*
3	4	5	0.4922
3	4	6	0.6657
3	4	7	0.7014
even	*even*	*even*	*1*
odd	*odd*	*odd*	*1*

Table 3: Equal mixtures of four energy states (n,m,q,r) for a single particle and a 50/50 partition. Italic (red online) text indicates states with quantum numbers which differ by >1.

n	m	q	r	EoF	n	m	q	r	EoF
1	2	3	4	0.2430	2	3	5	8	0.8558
1	2	3	5	0.5074	2	3	6	7	0.7316
1	2	3	6	0.4744	2	3	6	8	0.8551
1	2	4	5	0.4557	2	3	6	9	0.8585
1	2	4	6	0.5970	2	4	5	6	0.6388
1	2	4	7	0.6146	2	4	5	7	0.8603
1	2	5	6	0.4677	2	4	5	8	0.8428
1	2	5	7	0.6835	2	4	6	7	0.8560
1	2	5	8	0.6476	*2*	*4*	*6*	*9*	*0.9870*
1	3	4	5	0.5364	2	4	7	8	0.8055
1	3	4	6	0.6655	*2*	*4*	*7*	*9*	*0.9876*
1	3	4	7	0.7201	*2*	*4*	*7*	*10*	*0.9672*
1	3	5	6	0.7488	2	5	6	7	0.6254
1	*3*	*5*	*8*	*0.9524*	2	5	6	8	0.7702
1	3	6	7	0.8125	2	5	6	9	0.7884
1	*3*	*6*	*8*	*0.9296*	2	5	7	8	0.7794
1	*3*	*6*	*9*	*0.9419*	*2*	*5*	*7*	*9*	*0.9931*
1	4	5	6	0.5864	*2*	*5*	*7*	*10*	*0.9598*
1	4	5	7	0.8186	3	4	5	6	0.3689
1	4	5	8	0.7927	3	4	5	7	0.6039
1	4	6	7	0.7909	3	4	6	7	0.5840
1	*4*	*6*	*8*	*0.9293*	3	4	6	8	0.7323
1	*4*	*6*	*9*	*0.9262*	3	5	6	7	0.5805
1	4	7	8	0.7539	3	5	6	8	0.7222
1	*4*	*7*	*9*	*0.9463*	3	5	7	8	0.7708
1	*4*	*7*	*10*	*0.9196*	*3*	*5*	*7*	*10*	*0.9591*
2	3	4	5	0.4703	4	5	6	7	0.4551
2	3	4	6	0.6403	*4*	*7*	*9*	*11*	*0.9883*
2	3	4	7	0.6438	*4*	*6*	*8*	*11*	*0.9847*
2	3	5	6	0.6550	*odd*	*odd*	*odd*	*odd*	*1*
2	3	5	7	0.8948	*even*	*even*	*even*	*even*	*1*

In a similar manner, for mixtures of four or more states, the average entanglement of all contributing triples of states can be found. The comparison between the actual EoF and the pair-wise averages are displayed in figure 2 for the three and four state mixtures evaluated. Figure 2 also compares the actual EoF with the average over all triples for the four state mixtures. This figure shows that mixing does indeed reduce the entanglement in general. Averaging over the entanglements of the contributing triples produces a closer estimate than averaging over the contributing pairs, though it is still a significant over-estimate of the true entanglement. The poorer estimate of the entanglement obtained by pair-wise averaging for the four state mixtures, as compared with the three state mixtures, also illustrates the effect of increasing mixity in reducing the entanglement.

It is interesting that there appears to be an approximately linear relationship between the pair-wise averaged (or triple-averaged) entanglement and the true EoF, though this line varies according to the number of states in the mixture. This may provide a means of obtaining an accurate estimate of the EoF of any equal mixture of arbitrary quantum numbers (n,m,q,r…) provided that the EoF of the lowest energy state, (1,2,3,4…) is known. The latter provides the lowest point on the above lines, and hence provides the line itself [which also passes through the point (1,1)]. Of course, the EoF of all contributing two state mixtures must also be known – but this is computationally far easier.

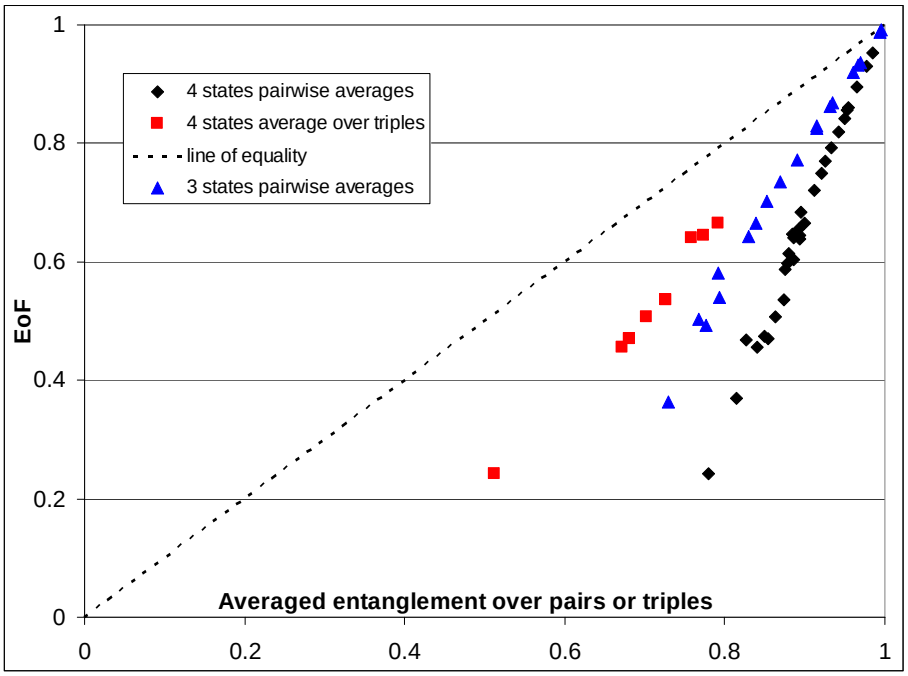

Figure 2. EoF of mixtures of 3 and 4 energy states for a single particle in a box: comparison with average entanglements of pairs and triples.

However, despite the general rule that mixing tends to decrease the entanglement, this does not mean that highly mixed states necessarily have small EoF. This is because it may be that every pair of states taken from a mixture has a large EoF, close to unity. This occurs if all the states have the same parity or if all pairs have a large difference in quantum number, $|n-m| >> 1$. In the latter case, table 1 indicates that the EoF of all pairs would be only slightly less than unity. Hence, the average EoF over all pairs would be close to unity and figure 2 implies that we may therefore expect the mixture itself to have large EoF, approaching 1. In particular, a mixture of an infinite number of equal parity states has both maximal mixity and maximal EoF, so that purity cannot always be used as an entanglement witness.

We have also studied equal mixtures of five, six, seven, eight, nine and ten distinct energy states. But in these cases we have confined attention to the mixtures with the lowest quantum numbers, 1, 2, 3… N_S, where N_S is 5, 6…10. From the preceding results we expect these states to have the smallest entanglement for each N_S value. The results are listed in table 4.

Table 4. Entanglement of equal mixtures with $n_i = i$.

n	Numerical EoF	Estimation Formulae, (26, 27)
2	0.3862	0.3645
3	0.3638	0.3495
4	0.2430	0.2430
5	0.2329	0.2329
6	0.1806	0.1823
7	0.1744	0.1748
8	0.1449	0.1458
9	0.1408	0.1398
10	0.1217	0.1215

These results suggest the following estimation formulae,

For even N_S: $$EoF = \frac{1.458}{2 + N_S} \quad (26)$$

For odd N_S: $$EoF = \frac{1.398}{1 + N_S} \quad (27)$$

These estimates are plotted in comparison with the numerically determined EoF in figure 3. The agreement is very good and seems to suggest that (26, 27) should provide a good extrapolation of the EoF to larger N_S values. If this extrapolation is indeed reliable, it suggests that the spatial EoF of a thermal state of a single particle will tend to zero at high temperatures. This is because the number of energy states which will contribute with comparable probabilities to a thermal mixture is of order $N_S \sim \sqrt{kT / E_1}$ where E_1 is the lowest energy state. Hence, the estimation formulae, (26,27), suggest that the single particle EoF will decrease $\propto 1/\sqrt{T}$ at sufficiently high temperatures in the 1D case.

The reduction of entanglement at increasing temperature conforms to expectation, [9,13,14,23,33,34]. However, given that mixity has been exposed as an unreliable guide to entanglement, this result is not as obvious as might have been supposed. In fact, the reason why a high temperature thermal state has vanishing entanglement is revealed to be, not merely due to its high mixity, but specifically because of the preponderance within the mixture of consecutive energy states, i.e. states differing in quantum number by 1. Although the numerical example has been carried out for box modes, the same conclusion must apply for any symmetrical potential which necessarily produces states of definite parity.

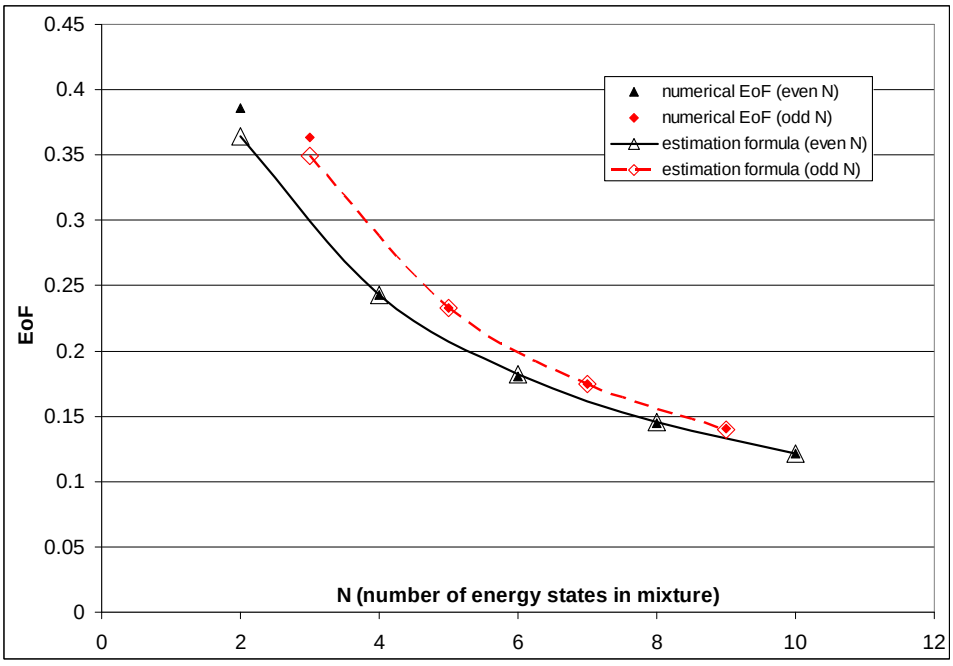

Figure 3. Numerical EoF compared with estimation formulae, (26,27), for equal mixed states of N consecutive energies (n,m,q,r… equal to 1,2,3,4…).

6. Mixtures approximating the thermal state of a single particle

In this Section we consider mixtures of the first ten consecutive energy states, but with unequal probabilities in the mixture. The probabilities are chosen to approximate a thermal state at temperature T, and a range of values of E_1 / kT are analysed from 0.001 to 2 (where E_1 is the ground state energy and k is Boltzmann's constant). Because we are using only 10 energy states, the mixture ceases to be an accurate representation of the thermal state when more than

10 states would contribute significantly to the true thermal mixture. The true thermal mixture would have probabilities relative to that of the ground state given by the Boltzmann factor (since we are considering states of just one particle the Bose distribution is not appropriate),

$$\frac{p_n}{p_1} = \exp\left\{-\frac{E_1}{kT}\left(n^2 - 1\right)\right\} \tag{28}$$

This is used as the basis for our assumed probabilities. However, the normalisation is adjusted to ensure the probabilities sum to unity over just the first 10 states. The approximation to the thermal state is expected to be reasonable for $kT \leq 30E_1$, for which the smallest contributing probability (p_{10}) is ≤0.05 times the largest (p_1).

The EoF was found using the numerical method described in the Appendix and the result for each temperature is shown in figure 4 (black curve) and in table 5. A surprise is that the case of equal probabilities does not produce the minimum EoF. Actually the minimum EoF occurs for the unequal probabilities labelled $E_1 / kT = 0.01$, see table 5, for which p_1 exceeds p_{10} by about x2.7 (though this case is not a good representation of a thermal state).

However, for $E_1 / kT \geq 0.03$, where the approximation to the thermal state is good, the behaviour of the EoF is as expected. At temperatures $kT < E_1/2$ the thermal state approximates to just ground state occupation, and hence the EoF becomes unity. However, at higher temperatures the EoF reduces steadily. It is clear from the graph that the EoF is tending towards zero at high temperature – until the limitation imposed by our restriction to just 10 states limits the accuracy of the representation of the thermal state. A power law fit suggests $EoF \propto T^{-0.63}$ for one particle in 1D when kT is sufficiently larger than E_1. This is not too different from the rough estimate that $EoF \propto 1/\sqrt{T}$ made in Section 5.3.

Table 5. Entanglement of 10-state mixtures approximating the thermal state of a single particle at various temperatures (50/50 partition).

E_1 / kT	EoF
0	*0.1217*
0.001	0.1184
0.01	0.1020
0.03	0.1167
0.05	0.1492
0.1	0.2235
0.2	0.3471
0.4	0.5578
0.6	0.7211
0.8	0.8331
1	0.9035
1.3	0.9591
1.6	0.9831
2	0.9949

7. The EoF of N-particle pure states of equal energy

The remainder of the paper addresses the spatial EoF of states of more than one particle, assumed to be bosons. In this Section we consider N bosons all in the same energy state. The following Sections consider states of two and three bosons in different energy states. Before proceeding, it is worth noting a potential source of confusion. Since the bosons are non-interacting, it may be tempting to equate the density matrix for N particles to the direct product of N one-particle density matrices, $\hat{\rho}_N = \rho_1^{\otimes N}$ An expression like this cannot apply in a site-based representation. The site-based partition can be regarded as expressing all states as a superposition of direct products of N_L

site states of the form $\prod_{i=1}^{N_L} \otimes |n\rangle_i$, where n is the occupancy of the i[th] lattice site. Whether the state in question is of one particle or many, the basis states are still direct products of the fixed number, N_L, of lattice sites. In this site-based partition an N particle state cannot be regarded as a direct product of one particle states, since an N particle state is also expressed in a basis of products of just N_L site-states.

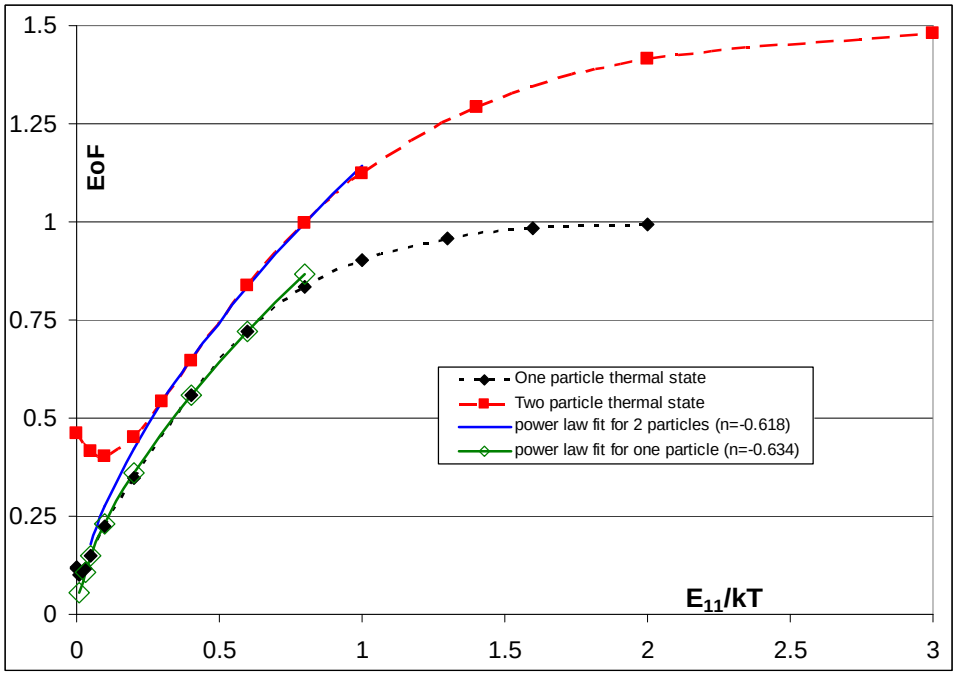

Figure 4. EoF for thermal states of one and two bosons compared. The representation of the thermal state becomes poor for $E_1/kT < 0.03$ for one particle, and for $E_{11}/kT < 0.2$ for two particles, but the extrapolation to zero entanglement at high temperature is clear (as illustrated by the T^{-n} fits).

The state of N particles all in the same energy state, n, can be decomposed into A,B partitioned states as follows,

$$\begin{aligned} |N(n)\rangle &= \frac{\left(\hat{a}_n^+\right)^N}{\sqrt{N!}}|0\rangle = \frac{\left(\alpha_k^A \hat{a}_{Ak}^+ + \alpha_k^B \hat{a}_{Bk}^+\right)^N}{\sqrt{N!}}|0\rangle \\ &= \frac{1}{\sqrt{2^N N!}} \sum_{r=0}^{N} \frac{N!}{r!(N-r)!} \left(\hat{a}_{Ak}^+\right)^r \left(\hat{a}_{Bk}^+\right)^{N-r} |0\rangle \\ &= \frac{1}{\sqrt{2^N N!}} \sum_{r=0}^{N} \frac{N!}{r!(N-r)!} \sqrt{r!}\sqrt{(N-r)!}\, |r(n)\rangle_A |N-r,(n)\rangle_B \\ &= \frac{1}{\sqrt{2^N}} \sum_{r=0}^{N} \sqrt{\frac{N!}{r!(N-r)!}}\, |r(n)\rangle_A |N-r,(n)\rangle_B \end{aligned} \tag{29}$$

where we have assumed the 50/50 box partition after the first line, and hence $\left|\alpha_k^{A,B}\right|^2 = ½$. This expression has previously been derived in [11]. Note that although the formalism has been explicitly written in 1D, by regarding the quantum numbers, n, k, etc., to be replaced by triples such as (n_x, n_y, n_z), etc., the same expression also applies for an N particle state of equal energies in

3D. The EoF of these pure states is found simply from the von Neumann entropy of the reduced density matrix. For example, for 2, 3 and 4 particles, the reduced density matrices are $diag(1,2,1)/4$, $diag(1,3,3,1)/8$ and $diag(1,4,6,4,1)/16$ and hence the EoFs are 1.5, 1.811 and 2.031 ebits respectively. Recall that the spatial EoF for a single particle energy state with a 50/50 partition is one ebit. Consequently, the EoF per particle of an N-particle state of equal energies diminishes as N grows.

The EoF for up to a million bosons was evaluated. A very good fit for the whole range of particle numbers is,

$$EoF = 1 + \log_2(\sqrt{N}) \tag{30}$$

The dependence on $\log_2(\sqrt{N})$ for large N can be derived from the Gaussian approximation to the binomial coefficients. The eigenvalues of the reduced density matrix are seen to be,

$$\lambda_r^N = \frac{{}_N C_r}{2^N} \approx \sqrt{\frac{2}{\pi N}} \exp\left\{-\frac{2m^2}{N}\right\}, \text{ where, } m = r - N/2 \tag{31}$$

and,

$$EoF = -\sum_{r=0}^{N} \lambda_r^N \log_2\left(\lambda_r^N\right) \tag{32}$$

The limiting dependence on N follows by noting that the width of the peak of (31) varies as $\sqrt{N}$, whereas the height of the peak (at m = 0) varies as $1/\sqrt{N}$. Consequently, the number of eigenvalues which make a significant contribution to the EoF is proportional to $\sqrt{N}$, and the magnitude of each is roughly proportional to $1/\sqrt{N}$. Hence, for large N the EoF will vary as,

$$EoF \to -\sqrt{N} \times \frac{1}{\sqrt{N}} \log_2\left(\frac{1}{\sqrt{N}}\right) = \log_2 \sqrt{N} \tag{33}$$

8. The EoF of two-particle pure states of unequal energy

The two-particle state comprising particles with energy quantum numbers n and m with $n \neq m$ is given, for a 50/50 partition, by,

$$|nm\rangle = \hat{a}_n^+ \hat{a}_m^+ |0\rangle = \frac{1}{2}\left(\hat{a}_{An}^+ + \hat{a}_{Bn}^+\right)\left(\hat{a}_{Am}^+ + \hat{a}_{Bm}^+\right)|0\rangle \tag{34}$$

Recalling the normalisation factors of (9,11) this two-particle state becomes,

$$|nm\rangle = \frac{1}{2}\left[\xi_{nm}|0\rangle_A|nm\rangle_B + |n\rangle_A|m\rangle_B + |m\rangle_A|n\rangle_B + \xi_{nm}|nm\rangle_A|0\rangle_B\right] \tag{35}$$

Because the one-mode states $|n\rangle_A$ and $|m\rangle_A$ are not orthonormal, we need to apply an orthonormalizing procedure to (35). The procedure is just as described in Section 5.1 and leads to,

$$|nm\rangle = \frac{1}{2}\left[\xi_{nm}|0\rangle_A|nm\rangle_B + C_{22}^B|n\rangle_A|\chi_2^B\rangle + C_{22}^A|\chi_2^A\rangle|n\rangle_B + \xi_{nm}|nm\rangle_A|0\rangle_B\right] \tag{36}$$

where the C-coefficients are found as in Section 5.1. Note that the derivation of (36) requires $C_{21}^A + C_{21}^B = S_{nm}^A + S_{nm}^A = 2\left(\int_{x\in A} + \int_{x\in B}\right) u(n,x)u^*(m,x)dx = 0$. Also note that correct normalisation of (36) follows from $|\xi_{nm}|^2 + |C_{22}^A|^2 = 1 + |S_{nm}^A|^2 + \left[1 - |S_{nm}^A|^2\right] = 2$ which follow from (11,23,25).

Equation (36) is a special case of a 4x4 bipartite state, the basis being $|0\rangle_A, |n\rangle_A, |\chi_2^A\rangle$ and $|nm\rangle_A$, and similar B-states. The reduced density matrix is obvious from (36), and diagonal. Putting

$\lambda = \left|S^A_{nm}\right|^2 = \left|S^B_{nm}\right|^2$ for a 50/50 partition gives the EoF of the most general pure state of two identical bosons with differing energies to be,

$$EoF = S_{vN}(\hat{\rho}_A) = -2\left[\left(\frac{1+\lambda}{4}\right)\log_2\left(\frac{1+\lambda}{4}\right) + \left(\frac{1-\lambda}{4}\right)\log_2\left(\frac{1-\lambda}{4}\right)\right] \tag{37}$$

In the case of equal parity states, we have λ = 0, since in this case the states are orthogonal on each half box. In this case the EoF achieves its maximum value of 2 ebits. Thus, each particle can be thought of as contributing unit entanglement.

For other choices of n and m the EoF is smaller because λ is non-zero. The largest value of λ occurs for n,m = 1,2, and is λ = 0.7208 for box confinement. Hence, the smallest EoF for any pure state of two particles in a box with different energy quantum numbers is 1.5832 ebits (with respect to a half & half partition). Note that the EoF for the case $n = m$, derived in Section 7, is 1.5 ebits, so the EoF for $n \neq m$ always exceeds that for $n = m$.

9. The EoF of three-particle pure states of unequal energy

The three particle case requires more effort than the two particle case because it turns out that we need to carry out an orthonormalizing procedure for four different states: two one-particle states and two two-particle states. For the 50/50 partition we have,

$$\left|nmq\right\rangle = \hat{a}^+_n\hat{a}^+_m\hat{a}^+_q\left|0\right\rangle = \frac{1}{2\sqrt{2}}\left(\hat{a}^+_{An} + \hat{a}^+_{Bn}\right)\left(\hat{a}^+_{Am} + \hat{a}^+_{Bm}\right)\left(\hat{a}^+_{Aq} + \hat{a}^+_{Bq}\right)\left|0\right\rangle \tag{38}$$

Hence,

$$\left|nmq\right\rangle = \frac{1}{2\sqrt{2}}\begin{bmatrix} \xi^B_{nmq}\left|0\right\rangle_A\left|nmq\right\rangle_B + \xi^A_{nmq}\left|nmq\right\rangle_A\left|0\right\rangle_B + \\ \xi_{mq}\left|n\right\rangle_A\left|mq\right\rangle_B + \xi_{nq}\left|m\right\rangle_A\left|nq\right\rangle_B + \xi_{nm}\left|q\right\rangle_A\left|nm\right\rangle_B + \\ \xi_{mq}\left|mq\right\rangle_A\left|n\right\rangle_B + \xi_{nq}\left|nq\right\rangle_A\left|m\right\rangle_B + \xi_{nm}\left|nm\right\rangle_A\left|q\right\rangle_B \end{bmatrix} \tag{39}$$

where the coefficients ξ_{ij} and $\xi^{A,B}_{nmq}$ are given by (11,12), and we note that $\xi^B_{nmq} = \xi^A_{nmq}$ for the 50/50 partition, so we can drop the superscript. The orthonormalization of the one-particle states proceeds as before. The orthonormalizing procedure for the two-particle states is as follows. Put,

$$\left|nq\right\rangle_A = D^A_{21}\left|nm\right\rangle_A + D^A_{22}\left|\theta^A_2\right\rangle \tag{40}$$

which defines the new orthogonalized state $\left|\theta^A_2\right\rangle$. Hence,

$$D^A_{21} = {}_A\!\left\langle nm\middle|nq\right\rangle_A = \left\langle 0\middle|\hat{a}_{Am}\hat{a}_{An}\hat{a}^+_{An}\hat{a}^+_{Aq}\right|0\rangle \tag{41}$$

Repeatedly applying the commutation relations, (7), results in,

$$D^A_{21} = \left[S^A_{mq} + S^A_{nm}S^A_{nq}\right]/\,\xi_{nm}\xi_{nq} \tag{42}$$

and,

$$D^A_{22} = \sqrt{1 - \left|D^A_{21}\right|^2} \tag{43}$$

Finally put,

$$\left|mq\right\rangle_A = D^A_{31}\left|nm\right\rangle_A + D^A_{32}\left|\theta^A_2\right\rangle + D^A_{33}\left|\theta^A_3\right\rangle \tag{44}$$

This defines the orthogonalized state $\left|\theta^A_3\right\rangle$ (together with the B-equivalent). The first coefficient follows from (42),

$$D_{31}^{A} = {}_{A}\langle nm|mq\rangle_{A} = \left[S_{nq}^{A} + S_{nm}^{A} S_{mq}^{A}\right] / \xi_{nm}\xi_{mq} \tag{45}$$

Using the definition of $\left|\theta_2^A\right\rangle$ from (40) gives,

$$D_{32}^{A} = {}_{A}\left\langle\theta_2^A\right|mq\rangle_{A} = \left[{}_{A}\langle nq|mq\rangle_{A} - D_{21}^{A} D_{31}^{A}\right] / D_{22}A \tag{46}$$

where,
$${}_{A}\langle nq|mq\rangle_{A} = \left[S_{nm}^{A} + S_{nq}^{A} S_{mq}^{A}\right] / \xi_{nq}\xi_{mq} \tag{47}$$

and finally,
$$D_{33}^{A} = \sqrt{1 - \left|D_{31}^{A}\right|^2 - \left|D_{32}^{A}\right|^2} \tag{48}$$

It is understood that (40-48) also apply with A replaced by B. We can now express (39) in terms of the orthonormalized states. The result is,

$$|nmq\rangle = \frac{1}{2\sqrt{2}} \left[\begin{array}{l} \xi_{nmq}|0\rangle_A|nmq\rangle_B + \xi_{nmq}|nmq\rangle_A|0\rangle_B + \\ \left[\xi_{mq}D_{31}^{B} + \xi_{nq}C_{21}^{A}D_{21}^{B} + \xi_{nm}C_{31}^{A}\right]n\rangle_A|nm\rangle_B + \\ \left[\xi_{mq}D_{31}^{A} + \xi_{nq}C_{21}^{B}D_{21}^{A} + \xi_{nm}C_{31}^{B}\right]nm\rangle_A|n\rangle_B + \\ \left[\xi_{mq}D_{32}^{B} + \xi_{nq}C_{21}^{A}D_{22}^{B}\right]n\rangle_A\left|\theta_2^B\right\rangle + \\ \left[\xi_{mq}D_{32}^{A} + \xi_{nq}C_{21}^{B}D_{22}^{A}\right]\left|\theta_2^A\right\rangle|n\rangle_B + \\ \left[\xi_{nq}C_{22}^{A}D_{21}^{B} + \xi_{nm}C_{32}^{A}\right]\left|\chi_2^A\right\rangle|nm\rangle_B + \\ \left[\xi_{nq}C_{22}^{B}D_{21}^{A} + \xi_{nm}C_{32}^{B}\right]nm\rangle_A\left|\chi_2^B\right\rangle + \\ \xi_{mq}D_{33}^{B}|n\rangle_A\left|\theta_3^B\right\rangle + \xi_{nq}C_{22}^{A}D_{22}^{B}\left|\chi_2^A\right\rangle\left|\theta_2^B\right\rangle + \xi_{nm}C_{33}^{A}\left|\chi_3^A\right\rangle|nm\rangle_B + \\ \xi_{mq}D_{33}^{A}\left|\theta_3^A\right\rangle|n\rangle_B + \xi_{nq}C_{22}^{B}D_{22}^{A}\left|\theta_2^A\right\rangle\left|\chi_2^B\right\rangle + \xi_{nm}C_{33}^{B}|nm\rangle_A\left|\chi_3^B\right\rangle \end{array}\right] \tag{49}$$

Consider firstly the case when n, m, q all have the same parity. In this case all the S coefficients are zero, which means that all the ξ coefficients are 1 and $C_{ij}^{A,B} = D_{ij}^{A,B} = \delta_{ij}$. Hence the 2nd through the 7th lines in (49) are all zero, and the coefficients of all the remaining terms become 1. Hence (49) reduces to,

$$|nmq\rangle = \frac{1}{2\sqrt{2}} \left[\begin{array}{l} |0\rangle_A|nmq\rangle_B + |nmq\rangle_A|0\rangle_B + |n\rangle_A\left|\theta_3^B\right\rangle + \left|\chi_2^A\right\rangle\left|\theta_2^B\right\rangle + \left|\chi_3^A\right\rangle|nm\rangle_B + \\ \left|\theta_3^A\right\rangle|n\rangle_B + \left|\theta_2^A\right\rangle\left|\chi_2^B\right\rangle + |nm\rangle_A\left|\chi_3^B\right\rangle \end{array}\right] \tag{50}$$

This is a special case of an 8x8 bipartite state, the 8 states for each partition being $|0\rangle_A, |n\rangle_A, \left|\chi_2^A\right\rangle, \left|\chi_3^A\right\rangle, |nm\rangle_A, \left|\theta_2^A\right\rangle, \left|\theta_3^A\right\rangle$ and $|nmq\rangle_A$, i.e. three one-particle states, three two-particle states, one three-particle state and the vacuum. The reduced density matrix is simply $\left(\hat{\rho}_A\right) = Tr_B\left(|nmq\rangle\langle nmq|\right) = \mathrm{I}_{8x8}/8$. The EoF is thus 3 ebits. In fact, it is clear that for any pure state of N particles whose energy states are all different but all have the same parity, the EoF will be N ebits. This follows from expressions like (39) since, in this case, all the ξ coefficients are 1 and all the states are orthogonal since $C_{ij}^{A,B} = D_{ij}^{A,B} = \delta_{ij}$. This contrasts sharply with the case when all N particles are in the same energy state, for which the EoF is very close to $1 + \log_2\sqrt{N}$.

We now consider the case n, m, q = 1, 2, 3. Based on previous results we expect that this will produce the smallest EoF for a pure 3-particle state in which all the n, m, q are different. Equation (49) evaluates (for box states) to,

$$|123\rangle = \frac{1}{2\sqrt{2}}\begin{bmatrix} 1.4072\left[|0\rangle_A|123\rangle_B + |123\rangle_A|0\rangle_B\right]+ \\ 1.0588\left[|\chi_2^A\rangle|12\rangle_B - |12\rangle_A|\chi_2^B\rangle\right]+ \\ 0.7339\left[|1\rangle_A|\theta_3^B\rangle + |\theta_3^A\rangle|1\rangle_B\right]+ \\ 0.4871\left[|\chi_2^A\rangle|\theta_2^B\rangle + |\theta_2^A\rangle|\chi_2^B\rangle\right]+ \\ 0.3505\left[|\chi_3^A\rangle|12\rangle_B + |12\rangle_A|\chi_3^B\rangle\right] \end{bmatrix} \tag{51}$$

Note that states $|12\rangle$ and $|\chi_2\rangle$ occur twice each in (51) and will thus give rise to off-diagonal terms in the reduced density matrix. Labelling the states 1 through 8 in the order: $|0\rangle_A, |1\rangle_A, |\chi_2^A\rangle, |\chi_3^A\rangle, |12\rangle_A, |\theta_2^A\rangle, |\theta_3^A\rangle, |123\rangle_A$ the reduced density matrix evaluates to,

(52)

$$(\hat{\rho}_A) = Tr_B(|123\rangle\langle 123|) = \begin{pmatrix} .2475 & 0 & 0 & 0 & & & & \\ 0 & .0673 & 0 & 0 & & & & \\ 0 & 0 & .1698 & .0464 & & & & \\ 0 & 0 & .0464 & .0154 & & & & \\ & & & & .1555 & -.0645 & 0 & 0 \\ & & & & -.0645 & .0297 & 0 & 0 \\ & & & & 0 & 0 & .0673 & 0 \\ & & & & 0 & 0 & 0 & .2475 \end{pmatrix}$$

The eigenvalues of (52) are 0.2475, 0.06733, 0.0025 and 0.18266, each being repeated. Hence the EoF of the state $|123\rangle$ is,

(53)

$$\begin{aligned} &EoF(|123\rangle) = S_{vN}(\hat{\rho}_A) \\ &= -2\{0.2475\log_2 0.2475 + 0.06733\log_2 0.06733 + 0.0025\log_2 0.0025 + 0.18266\log_2 0.18266\} \\ &= 2.461 \end{aligned}$$

Hence, the smallest EoF for any pure 3-particle state comprising different energy states is 2.461 ebits and thus exceeds the EoF of the pure 3-particle state with equal energies, which is 1.811 (see Section 7).

10. The EoF of two-particle thermal states

Consideration is restricted to mixtures of just 13 two-particle energy states, namely the states whose energy quantum numbers are (1,1), (1,2), (1,3), (1,4), (1,5), (2,2), (2,3), (2,4), (2,5), (3,3), (3,4), (3,5) and (4,4). This includes all states whose energy is 17 times the ground state, (1,1), energy or less. The density matrix is,

$$\hat{\rho} = \sum_{n,m} p_{nm}|n,m\rangle\langle n,m| \tag{54}$$

where (n,m) is summed over the 13 values indicated above. The probabilities, p_{nm}, are defined by the Boltzmann distribution,

$$\frac{p_{nm}}{p_{11}} = \exp\left\{-\frac{E_1}{kT}\left(\frac{n^2+m^2}{2}-1\right)\right\} \tag{55}$$

The probabilities are renormalized so that they sum to unity over the 13 states considered. It is expected that temperatures up to $kT/E_{11} \sim 5$ should be well represented by just 13 states, for which the smallest contributing probability (p_{12}) is $\leq 4\%$ of the largest (p_1). For higher temperatures our 13-state mixture will depart from the true thermal state. Each of the 13 pure two-particle states can be expressed in terms of partitioned states in one of two ways, depending upon whether n = m or $n \neq m$, thus,

n = m: $$\left|nn\right\rangle = \frac{1}{2}\left[\left|0\right\rangle_A\left|nn\right\rangle_B + \sqrt{2}\left|n\right\rangle_A\left|n\right\rangle_B + \left|nn\right\rangle_A\left|0\right\rangle_B\right] \tag{56}$$

$n \neq m$: $$\left|nm\right\rangle = \frac{1}{2}\left[\xi_{nm}\left\{\left|0\right\rangle_A\left|nm\right\rangle_{\mathbf{B}} + \left|nm\right\rangle_A\left|0\right\rangle_{\mathbf{B}}\right\} + \left|n\right\rangle_A\left|m\right\rangle_{\mathbf{B}} + \left|m\right\rangle_A\left|n\right\rangle_{\mathbf{B}}\right] \tag{57}$$

The main task we have in formulating the problem is to carry out the orthonormalizing process. This is required for both the one-particle partitioned states, $\left|n\right\rangle_{A,B}$, and also the two particle partitioned states, $\left|nm\right\rangle_{A,B}$, since neither are orthonormal as they stand. The five one-particle states, $\left\{\left|i\right\rangle_A, i = 1,2..5\right\}$, are orthonormalized precisely as described previously, the orthonormalized set of states being denoted $\left\{\left|\psi_i^A\right\rangle, i = 1,2..5\right\}$, where $\left|\psi_1^A\right\rangle \equiv \left|1\right\rangle_A$ and the remaining states are defined as in Section 5.1. Because (56,57) involve sums of products of one particle states, the numerical coefficients which finally appear are obtained as sums of products of the $C_{jk}^{A,B}$ coefficients of Section 5.1.

Orthonormalization of the two-particle states is similar and generalises the process already used in Section 9. There are 13 two-particle states for each partition, $\left|11\right\rangle_A, \left|12\right\rangle_A, \left|13\right\rangle_A, \left|14\right\rangle_A$, $\left|15\right\rangle_A, \left|22\right\rangle_A, \left|23\right\rangle_A, \left|24\right\rangle_A, \left|25\right\rangle_A$, $\left|33\right\rangle_A$, $\left|34\right\rangle_A, \left|35\right\rangle_A, \left|44\right\rangle_A$. These are to be expressed in terms of the orthonormalized states $\left\{\left|\theta_I^A, I = 1,2...13\right\rangle\right\}$, where $\left|\theta_1^A\right\rangle \equiv \left|11\right\rangle_A$, via the definitions,

$$\left|ij\right\rangle_A = \sum_{K=1}^{J} D_{JK}^A \left|\theta_K^A\right\rangle \tag{58}$$

where the capital indices take values in the range 1,2…13, labelling the two-particle states, and state J denotes (ij). With this notation, the D-coefficients are found from a similar formula to (24), i.e.,

for 1 < K < J, $$D_{JK}^A = \frac{1}{D_{KK}^{A*}}\left[{}_A\left\langle K\right|J\left\rangle_A - \sum_{I=1}^{K-1} D_{KI}^{A*} D_{JI}^A\right] \tag{59}$$

for K = 1, $$D_{J1}^A = {}_A\left\langle 1\right|J\left\rangle_A \tag{60}$$

where the two-particle scalar products, ${}_A\left\langle K\right|J\left\rangle_A$, are found from formulae depending upon which quantum numbers are common, i.e.,

$${}_A\left\langle nm\right|pq\left\rangle_A = \left[S_{np}^A S_{mq}^A + S_{nq}^A S_{mp}^A\right] / \xi_{nm}\xi_{pq} \tag{61}$$

$${}_A\left\langle nm\right|nq\left\rangle_A = \left[S_{mq}^A + S_{nm}^A S_{nq}^A\right] / \xi_{nm}\xi_{nq} \tag{62}$$

$${}_A\left\langle nm\right|qq\left\rangle_A = \sqrt{2} S_{nq}^A S_{mq}^A / \xi_{nm} \tag{63}$$

$${}_A\left\langle nq\right|qq\left\rangle_A = \sqrt{2} S_{nq}^A / \xi_{nq} \tag{64}$$

$$ {}_A\langle nn|qq\rangle_A = \left(S^A_{nq}\right)^2 \tag{65}$$

These expressions all follow from the commutation relations, (7). The final coefficient is determined by normalisation,

$$ D^A_{JJ} = \sqrt{1 - \sum_{K=1}^{J-1} \left| D^A_{JK} \right|^2} \tag{66}$$

After some labour, the components of the density matrix, (54), can thus be found in terms of the orthonormal basis formed by the direct product of the 19 A-partition states, $|0\rangle_A$, $\left\{ \left|\psi^A_i\right\rangle, i = 1,2..5 \right\}$, $\left\{ \left|\theta^A_I\right\rangle, I = 1,2...13 \right\}$, with the B-partition equivalents. The resulting density matrix is of dimension 19 x 19 = 361, though its rank is, of course, only 13.

The EoF of thermal mixtures of these 13 two-particle energy eigenstates has been found using the numerical procedure described in the Appendix. The results are shown plotted against inverse temperature in figure 4 and compared with the EoF of the one-particle thermal states. The salient feature is that the EoF reduces with increasing temperature, at least so long as $E_1 / kT > 0.2$ when the representation of the thermal state is good.

Like the one particle case, a surprise is that the case of equal probabilities does not produce the minimum EoF. Actually the minimum EoF occurs for the unequal probabilities labelled $E_1 / kT = 0.1$, see table 6, for which p_1 exceeds the smallest probability, p_{12}, by about x5 (though this case is not a good representation of a thermal state).

Figure 4 shows that the EoF of the two-particle thermal state approaches 1.5 at low temperatures (when the mixture becomes the pure ground state and Section 7 has shown that the EoF is then 1.5). Comparison with the one-particle thermal state shows that the EoF is larger for two particles (at a given temperature). As the temperature is increased the EoF reduces steadily (until $E_1 / kT > 0.1$ when the representation of the thermal state becomes poor). A power law fit suggests $EoF \propto T^{-0.62}$ for two particles in 1D when kT is sufficiently larger than E_{11}. This is not too different from the rough estimate that $EoF \propto 1/\sqrt{T}$ made in Section 5.3, and is almost identical to the one-particle result of Section 6.

Table 6. Entanglement of 13-state mixtures approximating the thermal state of two particles at various temperatures (50/50 partition).

E_{11}/kT	EoF
p = $^1/_{13}$	0.4613
0.05	0.4147
0.1	0.4020
0.2	0.4504
0.3	0.5436
0.4	0.6457
0.6	0.8372
0.8	0.9966
1.0	1.1226
1.4	1.2911
2.0	1.4148
3.0	1.4809
∞	1.5

11. Conclusions

The dependence of the spatial EoF on the partitions' size and position, and the gap between the partitions, is an elementary consequence of the confined wavefunction shapes.

For mixed energy states of a single particle: (a)The EoF remains high even for large mixities if all contributing pairs of quantum numbers differ by more than 1, i.e. if $|n-m|>1$ for all pairs; (b)The EoF is maximal (unity) if all contributing states have the same parity, even for maximal mixity; (c)The implication is that infinite sub-mixtures of thermal states, with maximal mixity, can also have maximal EoF, even at high temperatures when the thermal state itself has vanishing entanglement. Hence, the reduction of EoF at high temperatures does not arise due to increasing mixity alone. Purity is not always a good guide to entanglement for arbitrary types of mixture. It is true that increasing mixity most often has the tendency to reduce entanglement, and this has been illustrated here. But this general rule fails if the states in question are suitably contrived, e.g. of equal parity.

The EoF of thermal states of one or two bosons was found to diminish monotonically with increasing temperature, as expected. For one or two particles in one dimension, the results suggest that $EoF \propto 1/T^{x}$ with x about 0.5 to 0.63 for *kT* sufficiently large compared with the ground state energy. However, given that mixity has been exposed as an unreliable guide to entanglement, this result is not as obvious as might have been supposed. In fact, the reason why a high temperature thermal state has vanishing entanglement is revealed to be, not merely due to its high mixity, but specifically because of the preponderance within the mixture of consecutive energy states, i.e. states differing in quantum number by 1.

For N identical, non-interacting bosons in the same energy state a good approximation to the EoF is $1+\log_2(\sqrt{N})$. This result provides an upper bound to the absolute EoF which can be expected from a BEC. Even a million atoms in the condensed phase produce an EoF of only 11 ebits. The increasingly dilute specific entanglement (EoF/N) in the thermodynamic limit suggests that spatial entanglement in a BEC may not be a practical source of entanglement experimentally.

The EoF for N identical, non-interacting bosons in a pure state with differing energies always exceeds that for equal energies. The upper bound for the EoF of N identical, non-interacting bosons in a pure state with differing energies is N ebits. This bound is realised in the case of states of equal parity. This suggests that fermions may be potentially a richer source of spatial entanglement than bosons.

Appendix A. Numerical determination of the EoF

The method of conjugate gradients was used. The particular procedure employed has been described in [36,37]. The method relies upon all possible decompositions, $\hat{\rho}=\sum_j p'_j|\phi_j\rangle\langle\phi_j|$, of a given density matrix being expressible in terms of a right-unitary transformation from some arbitrary initial decomposition, $\hat{\rho}=\sum_i p_i|\psi_i\rangle\langle\psi_i|$. In these expressions j runs from 1 to J whereas i runs from 1 to I where J ≥ I. The values of I or J are the cardinalities of the particular decompositions. Thus, there exists a right-unitary matrix U which connects the two decompositions, $|\tilde{\phi}_j\rangle=\sum_{i=1}^{I}U_{ji}|\tilde{\psi}_i\rangle$, where $U^{+}U=1_{IxI}$ and the tilde on the states denotes that these are the sub-normalized states defined by $|\tilde{\psi}_i\rangle=\sqrt{p_i}|\psi_i\rangle$, $|\tilde{\phi}_i\rangle=\sqrt{p'_i}|\phi_i\rangle$. To capture all possible decompositions the initial decomposition is taken to have cardinality equal to the rank of $\hat{\rho}$, i.e., I = r. Parameterizing all right-unitary matrices in some convenient manner thus provides a parameter space whose points are in one-to-one correspondence with the set of all possible decompositions. In our formulation we preferred to search a space of fixed cardinality,

starting with a decomposition defined by r non-zero vectors plus 'padding' by the required number of additional zero vectors. (All 'J' vectors will subsequently become non-zero in general). The possibility of improved minima of different cardinality was explored by running the program separately for different cardinalities. The advantage of this is that the matrices, U, are then square, and hence unitary, and can be expressed in terms of an Hermetian matrix, Θ, as $U = \exp\{i\Theta\}$.

The problem is to find a point in this parameter space which minimises $E_{av} = \sum_i p_i' EoF(|\phi_i\rangle)$.

The basic strategy is to evaluate the gradient of E_{av} in parameter space and then to move in parameter space such that E_{av} reduces as quickly as possible. The obvious algorithm, to move along the negative gradient, produces the method of steepest descents. The method of conjugate gradients is a refinement of this which generally improves the rate of convergence. The expression for the gradient of E_{av} was taken from [37], equation (10), which gives,

$$dE_{av} = \sum_{i,j} g_{ji} d\Theta_{ij}, \text{ where, } g_{ji} = iTr_A\left\{\left[\log_2\left(\hat{\rho}_j^A\right) - \log_2\left(\hat{\rho}_i^A\right)\right] Tr_{\mathbf{B}}\left(\left|\tilde{\phi}_j\right\rangle\left\langle\tilde{\phi}_i\right|\right)\right\} \qquad \text{(A.1)}$$

where $\hat{\rho}_i = |\phi_i\rangle\langle\phi_i|$, $\hat{\rho}_i^A = Tr_B(\hat{\rho}_i)$ and $\mathrm{Tr}_{A,B}$ represent tracing-out the states of the indicated partition, e.g. $Tr_B(...) \equiv \sum_{x=B-states} {}_B\langle x|...|x\rangle_B$. Note that the gradient matrix, g, is evaluated at the current position in parameter space, i.e. in terms of the current (evolving) decomposition, $\left\{\left|\tilde{\phi}_j\right\rangle\right\}$. The bulk of the computational effort is expended in re-evaluating the gradient matrix at each new point, since its calculation requires eigenvalue extraction in order to find $\log_2\left(\hat{\rho}_i^A\right)$.

Some care is necessary since the JxJ real coordinates of the parameter space are not Θ_{ij}, since these are complex with $\Theta_{ij} = \Theta_{ji}^*$, but rather $\Re(\Theta_{ij})$ for i ≤ j and $\mathrm{Im}(\Theta_{ij})$ for i > j. Different variants of the conjugate gradient method involve different expressions for the conjugate gradient, specifically by how much it differs from the negative gradient. The Polak-Ribiere variant was employed here. In addition, a 'restart' was applied every N steps, with N set to the square of the rank. A 'restart' resets the conjugate gradient to the negative gradient. Finally, each step requires the line-minimum along the direction of the current conjugate gradient to be found. For this Brent's method was used.

A subtlety is that, for initial states of sufficient symmetry, the first order gradient can lead to only a sub-set of parameter space being explored. For example, if the coefficients of the input states are all real (as they are in this paper) then the above algorithm leads only to states with real coefficients, despite complex coefficients being essential to obtain the true minimum of E_{av} in most cases. In our implementation this problem was overcome by alternating the method of conjugate gradients with a simple search along prescribed curves in parameter space, a crude but effective strategy for symmetry breaking.

The major practical difficulty with non-linear optimisation is the distinction between a global minimum and a local minimum. Algorithms like the conjugate gradient method are attracted to local minima. In general there is no guarantee that this will be the global optimum. However, it has been suggested, [38], that local minima of E_{av} are also global minima. This is a major boon to the numerical determination of the EoF. It is easy to check that a local minimum has been reached, simply by evaluation of the finite differences in all coordinate directions. These should all be positive, but some components tend to be small and negative due to numerical limitations. A convergence parameter can be defined as the ratio of the algebraically smallest finite difference to the average value in all directions. This convergence parameter was of considerable utility in practice, further iterations being made until any negative value became suitably small in magnitude.

In passing we note that in all the cases reported here a cardinality equal to the rank of the density matrix was sufficient to obtain the minimum E_{av}, i.e. an optimal decomposition. This was demonstrated simply by trying larger cardinalities, but these never produced an improved minimum for our states. It is known that this is not always the case. Examples where the EoF is non-zero and the cardinality of the optimal decomposition exceeds the rank have been given in [32] and [36]. The latter example considers the so-called Horodecki 3x3 states, [39], whose rank is 7. The EoF of these states was evaluated numerically in [36]. The minimum was not obtained until a cardinality of 14, twice the rank, was used. We have repeated this exercise to test our numerical routines and confirm this result (and also that the magnitude of the EoF is very small, less than 0.01).

References

[1] Nielsen M A 1998 Quantum information theory *PhD dissertation University of New Mexico* (*Preprint* quant-ph/0011036)

[2] Bennett C H, Brassard G, Crepeau C, Jozsa R, Peres A, and Wootters W 1993 Teleporting an unknown quantum state via dual classical and EPR channels *Phys. Rev. Lett*. **70** 1895–99

[3] Bennett C H and Brassard G 1984 *Proc. IEEE Int. Conf. on Computers, Systems, and Signal Processing (Bangalore)* (New York), pp 175–179

[4] Ekert. A 1991 Quantum cryptography based on Bell's theorem *Phys. Rev. Lett.* **67** 661–63

[5] Bostrom K and Felbinger T 2002 Deterministic secure direct communication using entanglement *Phys. Rev. Lett.* **89** 187902 (*Preprint* quant-ph/0209040)

[6] Jozsa R 1997 Entanglement and quantum computation in *Geometric Issues in the Foundations of Science* ed S Huggett *et al* (Oxford University Press) (*Preprint* quant-ph/9707034)

[7] Nielsen M A and Chuang I L 2000 *Quantum Computation and Quantum Information* (Cambridge University Press)

[8] Einstein A, Podolsky B and Rosen N 1935 Can the quantum-mechanical description of physical reality be considered complete? *Phys. Rev.* **47**, 777–80

[9] Terra Cunha M O, Dunningham J A and Vedral V 2007 Entanglement in single particle systems *Proc. Royal Soc. Math & Phys.* **463** 2277-86 (*Preprint* quant-ph/0606149)

[10] Tommasini P, Timmermans E and de Toledo Piza A F R 1998 The hydrogen atom as an entangled electron-proton system *Am. J.Phys.* **66** 881

[11] Simon C 2002 Natural entanglement in Bose-Einstein condensates *Phys. Rev. A* **66** 052323 (*Preprint* quant-ph/0110114)

[12] Anders J, Kaszlikowski D, Lunkes C, Ohshima T and Vedral V 2006 Detecting entanglement with a thermometer *New J. Phys.* **8** 140 (*Preprint* quant-ph/0512181)

[13] Heaney L, Anders J, Kaszlikowski D and Vedral V 2007 Spatial entanglement from off-diagonal long range order in a BEC *Phys. Rev. A* **76** 053605 (*Preprint* quant-ph/0702067)

[14] Heaney L 2007 Entanglement in the Bose-Einstein condensate phase transition *Preprint* 0711.0942

[15] Peres A 1995 Nonlocal effects in Fock space *Phys. Rev. Lett.* **74** 4571

[16] Greenberger D M, Horne M A and Zeilinger A 1995 Nonlocality of a single photon? *Phys.Rev. Lett.* **75** 2064

[17] Santos E 1992 Comment on "Nonlocality of a single photon?" *Phys. Rev. Lett.* **68** 894

[18] Vaidman L 1995 Nonlocality of a single photon revisited again *Phys. Rev. Lett.* **75** 2063

[19] Bjork G, Jonsson P and Sanchez Soto L L 2001 Single-particle nonlocality and entanglement with the vacuum *Phys. Rev. A* **64** 042106 (*Preprint* quant-ph/0103074)

[20] Dunningham A and Vedral V 2007 Nonlocality of a single particle *Phys.Rev.Lett.* **99** 180404 (*Preprint* 0705.0322)

[21] Michler M, Weinfurter H and Zukowski M 2000 Experiments towards falsification of noncontextual hidden variable theories *Phys. Rev. Lett.* **84** 5457

[22] Osborne T J and Nielsen A 2002 Entanglement in a simple quantum phase transition *Phys.Rev. A* **66**, 032110 (*Preprint* quant-ph/0202162)

[23] Anders J 2008 Thermal state entanglement in harmonic lattices *Phys. Rev. A* **77** 062102 (*Preprint* 0803.1102)

[24] Heaney L and Anders J 2008 Bell-inequality test of spatial mode entanglement *Preprint* 0810.2882

[25] Popescu S and Rohrlich D 1997 Thermodynamics and the measure of entanglement *Phys. Rev. A* **56** R3319-21

[26] Vedral V, Plenio M B, Rippin M A and Knight P L 1997 Quantifying entanglement *Phys. Rev. Lett.* **78** 2275-9 (*Preprint* quant-ph/9702027)

[27] Adesso G, Illuminati F and de Siena S 2003 Characterizing entanglement with global and marginal entropic measures *Phys. Rev. A* **68** 062318 (*Preprint* quant-ph/0307192)

[28] Adesso G, Serafini A and Illuminati F 2004 Determination of continuous variable entanglement by purity measurements *Phys. Rev. Lett.* **92** 087901 (*Preprint* quant-ph/0310150)

[29] Bennett C H, DiVincenzo D P, Smolin J A and Wootters W K 1996 Mixed state entanglement and quantum error correction *Phys. Rev. A* **54** 3824-3851 (*Preprint* quant-ph/9604024)

[30] Hill S and Wootters W K 1997 Entanglement of a pair of quantum bits *Phys. Rev. Lett.* **78** 5022–5 (*Preprint* quant-ph/970304)

[31] Wootters W K 1998 Entanglement of formation of an arbitrary state of two qubits *Phys. Rev.Lett.* **80** 2245–8 (*Preprint* quant-ph/9709029)

[32] Terhal B M and Vollbrecht K G 2000 The entanglement of formation for isotropic states *Phys. Rev. Lett.* **85** 2625-8 (*Preprint* quant-ph/0005062)

[33] Heaney L, Anders J and Vedral V 2006 Spatial entanglement of a free bosonic field *Preprint* quant-ph/0607069

[34] Kaszlikowski D, Keil A, Wiesniak M and Willenboordse F H 2006 Spatial entanglement of bosons in thermal equilibrium *Preprint* quant-ph/0601089

[35] Vidal G and Werner R F 2002 Computable measure of entanglement *Phys.Rev. A* **65** 032314

[36] Audenaert K, Verstraete F and de Moor B 2001 Variational characterisations of separability and entanglement of formation *Phys. Rev. A* **64** 052304 (*Preprint* quant-ph/0006128)

[37] Gittings J R and Fisher A J 2003 An efficient numerical method for calculating the entanglement of formation of arbitrary mixed quantum states of any dimension *Preprint* quant-ph/0302018

[38] Prager T 2001 A necessary and sufficient condition for optimal decompositions *Preprint* quant-ph/0106030

[39] Horodecki P 1997 Separability criterion and inseparable mixed states with positive

partial transposition *Phys. Lett. A* **232** 333-9

[40] Hessmo B, Usachev P, Heydari H and Björk G 2004 Experimental demonstration of single photon nonlocality *Phys. Rev. Lett.* **92** 180401